

# Discrimination of Ligands with Different Flexibilities Resulting from the Plasticity of the Binding Site in Tubulin

Soumyananda Chakraborti,<sup>†</sup> Devlina Chakravarty,<sup>†</sup> Suvroma Gupta,<sup>‡</sup> Biswa Prasun Chatterji,<sup>§</sup> Gopa Dhar,<sup>†</sup> Asim Poddar,<sup>†</sup> Dulal Panda,<sup>§</sup> Pinak Chakrabarti,<sup>†,||</sup> Shubhra Ghosh Dastidar,<sup>\*,||</sup> and Bhabatarak Bhattacharyya<sup>\*,†</sup>

<sup>†</sup>Department of Biochemistry, Bose Institute, Kolkata 700054, India

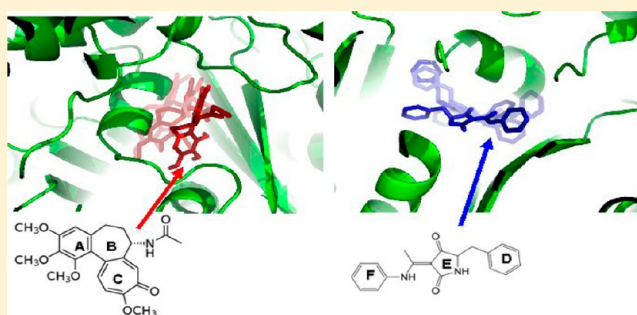
<sup>‡</sup>Department of Biotechnology, Haldia Institute of Technology, ICARE Complex, Purba Medinipur 721657, India

<sup>§</sup>Department of Biosciences and Bioengineering, Indian Institute of Technology Bombay, Mumbai 400076, India

<sup>||</sup>Bioinformatics Centre, Bose Institute, Kolkata 700054, India

## S Supporting Information

**ABSTRACT:** Tubulin, an  $\alpha\beta$  heterodimer, has four distinct ligand binding sites (for paclitaxel, peloruside/laulimalide, vinca, and colchicine). The site where colchicine binds is a promising drug target for arresting cell division and has been observed to accommodate compounds that are structurally diverse but possess comparable affinity. This investigation, using two such structurally different ligands as probes (one being colchicine itself and another, TN16), aims to provide insight into the origin of this diverse acceptability to provide a better perspective for the design of novel therapeutic molecules. Thermodynamic measurements reveal interesting interplay between entropy and enthalpy. Although both these parameters are favourable for TN16 binding ( $\Delta H < 0$ ,  $\Delta S > 0$ ), but the magnitude of entropy has the determining role for colchicine binding as its enthalpic component is destabilizing ( $\Delta H > 0$ ,  $\Delta S > 0$ ). Molecular dynamics simulation provides atomistic insight into the mechanism, pointing to the inherent flexibility of the binding pocket that can drastically change its shape depending on the ligand that it accepts. Simulation shows that in the complexed states both the ligands have freedom to move within the binding pocket; colchicine can switch its interactions like a “flying trapeze”, whereas TN16 rocks like a “swing cradle”, both benefiting entropically, although in two different ways. Additionally, the experimental results with respect to the role of solvation entropy correlate well with the computed difference in the hydration: water molecules associated with the ligands are released upon complexation. The complementary role of van der Waals packing versus flexibility controls the entropy–enthalpy modulations. This analysis provides lessons for the design of new ligands that should balance between the “better fit” and “flexibility”, instead of focusing only on the receptor–ligand interactions.



Microtubules are long, filamentous, tube-shaped protein polymers that are common to all eukaryotic cells, being a key component of the cytoskeleton. Microtubules are composed of  $\alpha\beta$  tubulin heterodimers (~50 kDa each). They control several important cellular functions, such as maintenance of cell shape, intracellular transport of vesicles, cell signaling, cell division, and mitosis.<sup>1</sup> In particular, the role in mitosis and cell division has been exploited to establish tubulin and microtubules as an attractive target for the development of anticancer drugs.<sup>2</sup> Such antimitotic drugs have been shown to bind specifically at one of the four major drug binding sites on tubulin, which are known as the paclitaxel, peloruside/laulimalide, vinca, and colchicine binding sites.<sup>3,4</sup> Among them, the binding of colchicine and vinca destabilizes the microtubule, while paclitaxel and peloruside/laulimalide binding stabilizes it. Although the paclitaxel and vinca alkaloids have exhibited clinical utility for the treatment of cancer, their

applications have been limited because of the rapid emergence of drug resistance.<sup>5</sup>

Colchicine, being the classic paradigm of an antimitotic drug, is one of the compounds used extensively to understand the properties and function of tubulin and microtubules in eukaryotic cells.<sup>1</sup> Colchicine binds at the interface of dimeric tubulin with high affinity, and the specificity of the drug–protein interaction is comparable to that of the enzyme–substrate reaction (Figure 1). Although colchicine generally binds to the tubulin dimer, there are reports showing its binding with the monomer. Banerjee et al. have earlier reported that colchicine can bind the tubulin monomer at a very low protein concentration (<0.2  $\mu\text{M}$ ) where its binding is faster and

Received: April 13, 2012

Revised: August 13, 2012

Published: August 14, 2012



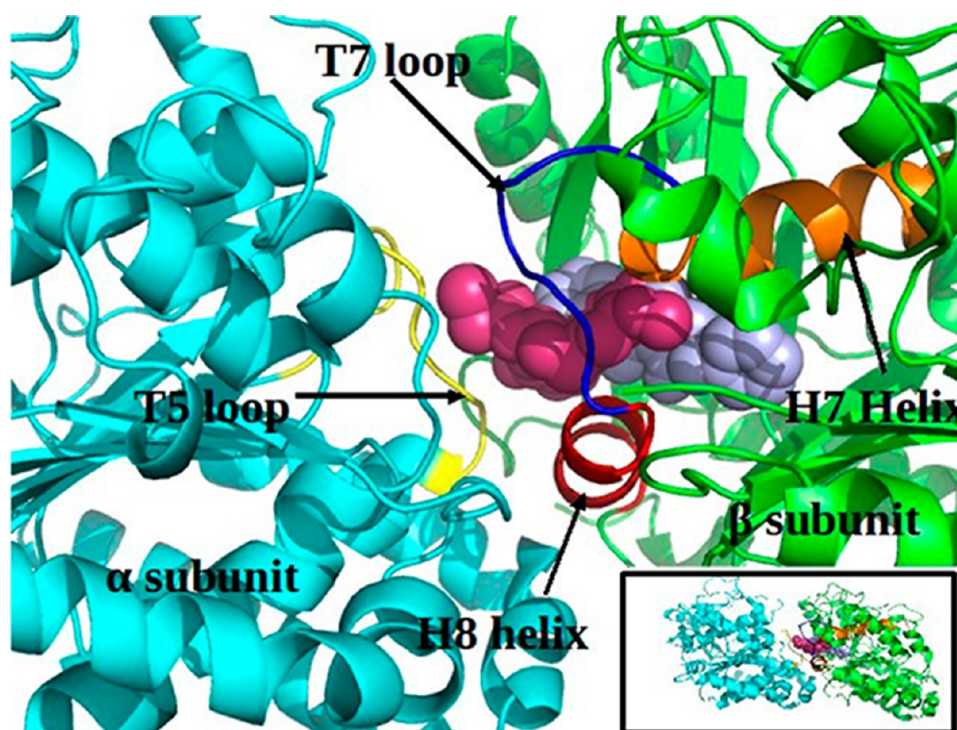


**Figure 1.** Cartoon representation showing an enlarged view of the colchicine binding site with the  $\alpha$  and  $\beta$  subunits colored cyan and green, respectively. The T5 (yellow) and T7 (blue) loops and H7 (orange) and H8 (red) helices and the two drugs, colchicine (pink spheres) and TN16 (slate blue spheres), are marked. The full structure of the dimer is depicted in the inset.

partially reversible.<sup>6</sup> The colchicine molecule is composed of three rings, a trimethoxy benzene ring (A-ring), a methoxy-tropone ring (C-ring), and a seven-member ring (B-ring) anchoring A- and C-rings and having an acetamido group at its C7 position (Figure 2). Although a large amount of binding

colchicine causes a total loss of the activity of the molecule.<sup>7</sup> An A-ring analogue alone, such as mescaline, binds tubulin with a very reduced affinity ( $\sim 10^3 \text{ M}^{-1}$ ).<sup>8</sup> Similarly, a C-ring analogue of methoxy-tropone also binds tubulin with a lower affinity.<sup>9</sup> A structure–activity study established that the presence of both A- and C-rings is the minimal structural requirement for its high-affinity binding to tubulin.<sup>10</sup> Thus, AC [2-methoxy-5-(2',3',4'-trimethoxyphenyl)tropone] is a colchicine analogue containing the minimal structural requirement that binds tubulin with a high affinity and elicits antimitotic activity.<sup>10–12</sup>

The essential structural requirement for the recognition of the C-ring is yet to be understood. In some cases, it is very stringent as observed in the case of isocolchicine (Figure 2).<sup>13</sup> Isocolchicine and colchicine share identical A-rings, while the relative positions of the methoxy and carbonyl groups in the C-ring are interchanged (Figure 2). This structural change generated an inactive analogue of colchicine. On the other hand, the replacement of the seven-membered tropone (C-ring) with a six-membered aromatic ring with a different substitution, such as allocolchicine, inhibits tubulin self-assembly.<sup>14</sup>

As mentioned earlier, the simplest colchicine analogue containing A- and C-rings constitutes the essential scaffold for tubulin binding.<sup>10–12</sup> AC has a more flexible structure, where the free movement of both A- and C-rings is possible. The addition of the B-ring, which anchors A- and C-rings, causes their immobilization, producing an analogue that is less flexible than AC. These structural changes as well as the addition of a side chain at position C7 affect the kinetics (on rate, off rate, activation energy, and reversibility)<sup>11,12,15–17</sup> and the thermodynamic properties (conformational entropy) of the binding interaction. On the other hand, a synthetic small molecule, termed TN16 (Figure 2), which targets the same binding site of colchicine, binds the tubulin dimer reversibly at

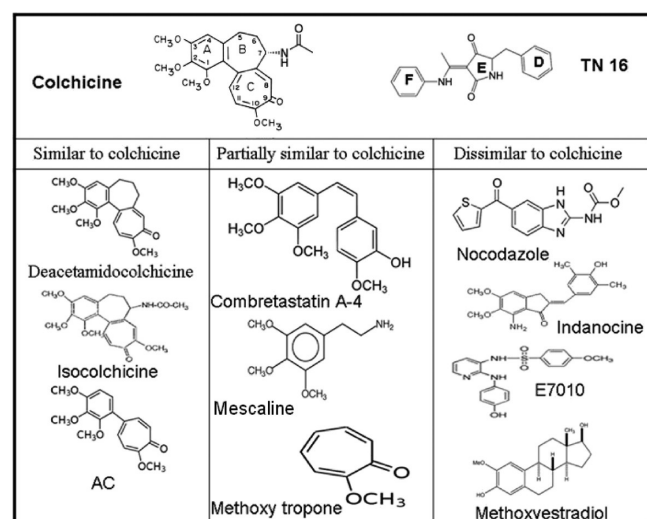


**Figure 2.** List of antimitotic compounds known to bind at the colchicine binding site.

data for different structural analogues of colchicine have been collected, the structural specificity of colchicine for its binding site at tubulin is not yet well understood. In the case of the A-ring, all three methoxy groups are crucial for tubulin binding and their substitution results in a many-fold reduction in potency.<sup>7</sup> Thus, the insertion of a sugar group into the A-ring of

30 °C; significant binding occurs even at 0 °C. The crystal structures of the complexes [Protein Data Bank (PDB) entries 1SA0 and 3HKD for tubulin–colchicine and tubulin–TN16 complexes, respectively] indicate that the ligands have different topology and coordination in the binding pocket.<sup>18</sup> TN16 has no notable structural resemblance with colchicine, yet it shares the binding site of colchicine. Interestingly, there are several other ligands that compete for the colchicine binding site, being structurally dissimilar to each other.<sup>19</sup> This observation is not only intriguing but also puzzling with respect to the empirical deduction of structural features for a better fitting ligand in the colchicine binding site.

Even though the colchicine binding site is the most studied of the four well-characterized drug binding sites of tubulin, the use of colchicine as a chemotherapeutic agent for the treatment of cancer suffers because of its toxicity at the effective drug concentrations.<sup>20</sup> It became a challenge for the drug discoverers to explore suitable molecules that will bind to the same site and cause less toxicity. The crystal structure of the tubulin–colchicine complex<sup>21</sup> provides the details of the pharmacophoric attachment points at the colchicine binding site. In fact, the drugs that target the colchicine binding site are currently undergoing intensive investigation as vascular targeting agents for cancer therapy.<sup>22,23</sup> There are other compounds that also target the colchicine binding site, but interestingly, they either possess only a partial structural similarity to colchicine or are completely dissimilar (Figure 2). Among the highly promising drugs, combrestatin possesses partial structural similarity to colchicine, whereas methoxyestradiol and E7010 are remarkably different; all of them are under clinical trials for their effectiveness as inhibitors.<sup>24,25</sup> The search for potential anticancer drugs targeting tubulin is at present a hot spot of research, striving for an understanding of the mechanism through which the drugs achieve their binding to the pocket, and the factors that tune the affinity.<sup>26</sup>

TN16 has long been recognized as a potential inhibitor of microtubule assembly.<sup>27</sup> Although the crystal structure of its complex with tubulin is known,<sup>18</sup> only limited information about the thermodynamics and binding mechanism is available. This study investigates the details of the interactions and the thermodynamics of binding, underpinning the critical differences employed in accommodating colchicine and TN16 in tubulin. The experimental data indicated a significant improvement in binding enthalpy that correlates with the deeper burial of TN16 relative to that of colchicine seen in the crystal structures (Table 1). For entropic stabilization, there must be a crucial role of motions both for the ligands and for the residues in the receptor that cannot be judged from the static structural model and requires the investigation of dynamics. The molecular dynamics (MD) of these structures have been simulated to investigate the characteristics of the ligand motions and the flexibility of the receptor pocket to

complement the experimental results for the rationalization of the role of entropy in the tubulin–drug interaction.

## METHODS

**Materials.** Colchicine, TN16, PIPES, EGTA, PMSF, DTT, GTP, glutamic acid, and glycerol were purchased from Sigma Aldrich (St. Louis, MO). All other reagents were of analytical grade, and doubly distilled water was used throughout the experiment.

**Tubulin Isolation and Estimation.** Tubulin was isolated from goat brains by two cycles of a temperature-dependent assembly and disassembly process. Briefly, tubulin with microtubule-associated proteins (MAPs) was isolated from crude brain extract by two cycles of polymerization using 4 M glycerol in PEM buffer with 1 mM GTP. Pure tubulin was then separated from MAPs by two additional cycles of polymerization by 1 M glutamate (GEM).<sup>28</sup> The protein was stored at –80 °C. The protein concentration was determined by the Lowry method using bovine serum albumin as the standard. Tubulin preparations used in this study contained a natural mixture of isoforms. Calorimetry measurements were taken with this unfractionated tubulin, and therefore, the binding parameters obtained here are averages for the different isoforms.<sup>29</sup>

**Isothermal Titration Calorimetry (ITC).** ITC was used to determine the thermodynamic parameters of tubulin–TN16 interactions. Tubulin was extensively dialyzed in PEM buffer in the presence of GDP (to offer stabilization), and the ligand (TN16) was dissolved in the last dialyzant. The pH of the tubulin and the ligand solutions was made identical before they were loaded into the calorimeter. A typical titration experiment involved 13 injections of ligand (20  $\mu$ L aliquots per shot), at 3 min intervals, into the sample cell (volume of 1.4359 mL) containing tubulin. The titration cell was kept at a constant temperature, and the contents were stirred continuously at 310 rpm. The data were then analyzed to determine the binding stoichiometry (*N*), affinity constant (*K<sub>a</sub>*), and thermodynamic parameters of the reaction, using Origin version 5.0.

**Computational Modeling and Simulation.** The starting structures for the simulation were taken from the Protein Data Bank (PDB): tubulin bound to TN16 (PDB entry 3HKD, 3.65 Å resolution) and tubulin bound to colchicine (PDB entry 1SA0, 3.5 Å resolution). Chains A and B of the tubulin heterodimer forming a complex with colchicine and TN16 were considered for the simulation. All calculations were performed using the Sander module of AMBER 10.<sup>30</sup> The parm99 force field was used, and the small molecules (colchicine and TN16) were parametrized using the ‘Antechamber’ module of AMBER. The Generalized Born Surface Area (GBSA) implicit solvent model was used with parameters described by Tsui.<sup>31</sup> Systems were energy minimized and then heated to 300 K, followed by equilibration. The production run was conducted using Langevin dynamics simulation for 10 ns each, for the complexed, uncomplexed, monomeric, and dimeric states as well as the uncomplexed ligands, whose details are listed in Table S1 of the Supporting Information. The nonbonded cutoff distance was set to 16 Å, and a 2 fs integration time step was used, applying SHAKE to freeze the vibrations of the bonds involving hydrogen. The coordinates were saved after each 2 ps. The figures are generated using Pymol (<http://www.pymol.org/>), and movies were prepared using VMD (<http://www.ks.uiuc.edu/Research/vmd/>). The solvent accessible surface area (ASA) was calculated using NACCESS ([\*\*Table 1. Thermodynamic Parameters for the Binding of Tubulin to TN16 and Colchicine at Room Temperature\*\*](http://www.bioinf.</a></p>
</div>
<div data-bbox=)

parameter	TN16	colchicine <sup>11,15</sup>
<i>N</i> (drug:protein stoichiometry)	0.86	~1
<i>K<sub>a</sub></i> (binding constant, M <sup>–1</sup> )	$2.1 \times 10^5 \pm 1 \times 10^4$	$1 \times 10^7 \pm 1 \times 10^5$
$\Delta H$ (kcal/mol)	$-1.7 \pm 0.58$	10.0
$T\Delta S$ (kcal/mol)	5.7	19.6
$\Delta G$ (kcal/mol)	–7.4	–9.6



manchester.ac.uk/naccess/) and POPS (Parameter Optimised Surfaces)<sup>32</sup> web server (<http://www.cs.vu.nl/~ibivu/programs/popswww>). The cavity analysis and visualization were conducted using CASTp (Computer Atlas of Surface Topography of proteins)<sup>33</sup> (<http://sts.bioengr.uic.edu/castp/calculation.php/>).

## RESULTS

**Thermodynamics of Tubulin–TN16 Interaction.** The thermodynamics of tubulin–colchicine binding are available in literature and are summarized in Table 1. In brief, colchicine binding ( $\Delta G \sim -9.6$  kcal/mol) is dominated by the entropic term ( $T\Delta S = 19.6$  kcal/mol), as the enthalpy of binding is unfavorable ( $\Delta H > 0$ ).<sup>11,15</sup> The complexation reaction for tubulin–TN16 interaction was found to be exothermic in nature (Figure 3a), and the values of the binding free energy

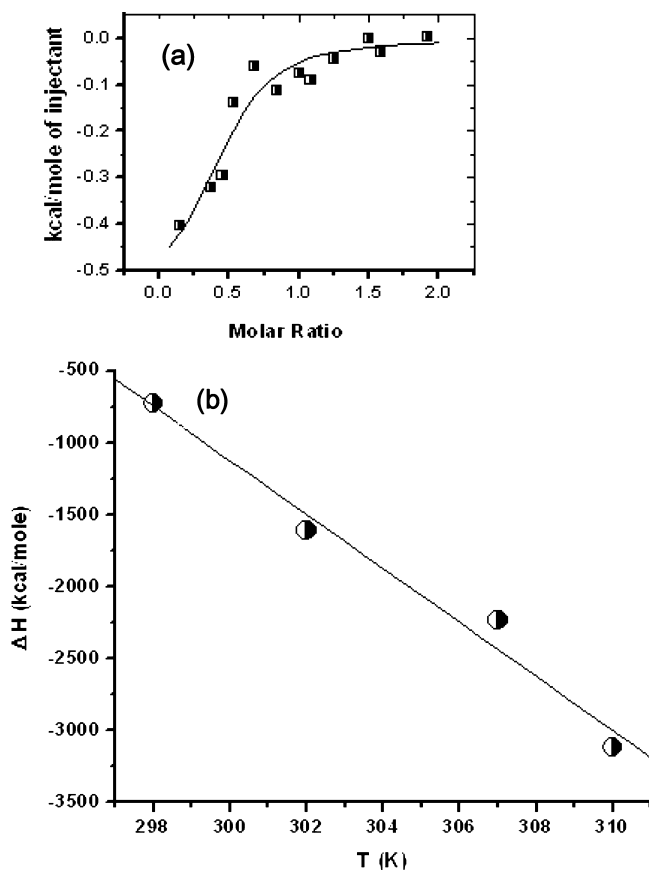


**Figure 3.** Titration of tubulin with TN16 by ITC. (a) Heat evolved per mole of TN16 vs the molar ratio (ligand:tubulin) for each injection. The titration was conducted in 50 mM PEM buffer (pH 7). (b) Temperature dependence of the enthalpy change ( $\Delta H$ ) of tubulin–TN16 interaction.

( $\Delta G$ ) and the equilibrium constant ( $K_a$ ) (Table 1) indicate moderate binding ( $\Delta G \sim -7.4$  kcal/mol). A plot of the change in enthalpy ( $\Delta H$ ) of tubulin–TN16 binding as a function of temperature (Figure 3b) yields a heat capacity change ( $\Delta C_p$ ) of  $-0.19$  kcal mol<sup>-1</sup> K<sup>-1</sup> (Table 2). For the formation of a complex (e.g., protein–protein, protein–ligand, etc.),  $\Delta C_p$  is usually negative, as these types of interactions are associated with the burial of surface at the interface of binding and thus the removal of interfacial water.<sup>34</sup> Reflecting a similar mechanism, the negative value of  $\Delta C_p$  observed for TN16

**Table 2.** Effect of Temperature on Different Thermodynamic Parameters of TN16 Binding; Experimental (exptl) and Calculated (calcd)

temp (K)	$\Delta H$ (kcal/mol)	$T\Delta S$ (kcal/mol)	$\Delta C_p^{\text{exptl}}$ (kcal mol <sup>-1</sup> K <sup>-1</sup> )	$\Delta C_p^{\text{calcd}}$ (kcal mol <sup>-1</sup> K <sup>-1</sup> )
298	-0.7	-6.5	-0.19	-0.24
302	-1.7	-5.7		
307	-2.2	-4.6		
310	-3.1	-3.8		

indicates that it is associated with a large degree of surface–surface association (between the protein and the drug), or a change in structural packing that results in the change in surface area. The estimation of  $\Delta C_p$  for binding of colchicine to tubulin could not be measured by ITC because tubulin–colchicine interaction is very slow (poor on rate) and the equilibrium is difficult to achieve after each addition of colchicine during the titration. Therefore, the equation by Murphy et al. was adopted to empirically calculate the  $\Delta C_p$  for this system.<sup>35</sup>

$$\Delta C_p = \Delta c_{np} \Delta ASA_{np} + \Delta c_p \Delta ASA_p \quad (1)$$

where  $\Delta C_p$  has two components, one positive and one negative; the positive component arises from the burial of polar surfaces ( $\Delta ASA_p$ ), whereas the negative component results from burial of apolar surfaces ( $\Delta ASA_{np}$ ). The accessible surface area (ASA) is defined as the surface generated by rolling a probe (a sphere with a radius of 1.4 Å) over the protein structure.<sup>36</sup> The equation also includes  $\Delta c_p$  and  $\Delta c_{np}$ , which are empirically determined coefficients of  $\Delta ASA_p$  and  $\Delta ASA_{np}$  with values of  $0.43 \times 10^{-3}$  and  $-0.26 \times 10^{-3}$  kcal/K, respectively.<sup>37</sup> Following eq 1, the  $\Delta C_p$  for the tubulin–colchicine interaction was found to be  $-0.28$  kcal mol<sup>-1</sup> K<sup>-1</sup>, which is more negative than the experimental value ( $-0.19$  kcal mol<sup>-1</sup> K<sup>-1</sup>) for the tubulin–TN16 complex (Table 2). For the latter complex, the theoretical  $\Delta C_p$  value ( $-0.24$  kcal mol<sup>-1</sup> K<sup>-1</sup>) closely resembles the experimental one, the variation being within the permissible range.<sup>37</sup>

In the uncomplexed state, colchicine possesses a relatively rigid structure, while TN16 has a flexible configuration (Movies SM1 and SM2 of the Supporting Information), in which the free rotations of both rings are feasible. The structural flexibility of a molecule largely determines the kinetics (on rate vs off rate) and the energetics of protein–drug interaction. Good examples of such consequences are tubulin–TN16 and –AC interactions. It is reported that AC binds tubulin instantaneously and reversibly,<sup>12</sup> and the binding occurs even at a very low temperature (0 °C). Thermodynamic components of protein–drug binding are largely modulated by the flexibility of the ligand molecule, and it has been demonstrated that for a flexible ligand conformational entropy terms could make the most significant contribution.<sup>38</sup> Such a possibility has been investigated for colchicine and TN16 by estimating the conformational entropy in the following way. The total entropic contribution associated with a binding reaction can be expressed as the sum of three terms.<sup>37,39</sup>

$$\Delta S_{\text{tot}} = \Delta S_{\text{conf}} + \Delta S_{\text{solv}} + \Delta S_{\text{r/t}} \quad (2)$$

where  $\Delta S_{\text{solv}}$  represents the change in entropy resulting from solvent release upon binding,  $\Delta S_{\text{conf}}$  is the configurational term reflecting the change in conformational fluctuations of the molecular structures, and  $\Delta S_{\text{r/t}}$  describes the loss of translational and rotational degrees of freedom when a complex is

**Table 3. Deconstruction of the Entropic Term (in kilocalories per mole per kelvin) into Its Components for the Binding of TN16, Colchicine, and Indanocine to Tubulin**

drug	$\Delta C_p$	$\Delta S_{\text{tot}}$	$\Delta S_{\text{r/t}}$	$\Delta S_{\text{solv}}$	$\Delta S_{\text{conf}}$
TN16 (exptl)	−0.19	$21.6 \times 10^{-3}$	$-8 \times 10^{-3}$	$48.1 \times 10^{-3}$	$-18.4 \times 10^{-3}$
TN16 (calcd)	−0.24	$21.6 \times 10^{-3}$	$-8 \times 10^{-3}$	$61.5 \times 10^{-3}$	$-31.9 \times 10^{-3}$
colchicine (calcd)	−0.28	$60 \times 10^{-3}$	$-8 \times 10^{-3}$	$72.1 \times 10^{-3}$	$-4.1 \times 10^{-3}$
indanocine (exptl) <sup>42</sup>	−0.18	$16.3 \times 10^{-3}$	$-8 \times 10^{-3}$	$44.8 \times 10^{-3}$	$-20.5 \times 10^{-3}$

<sup>a</sup>Values for colchicine and TN16 (calcd) are based on the calculation of ASA.

formed from two molecules free in solution. The numerical value of  $\Delta S_{\text{r/t}}$  is close to the critical entropy of  $-8 \times 10^{-3}$  kcal mol<sup>−1</sup> K<sup>−1</sup>.<sup>40</sup>  $\Delta S_{\text{solv}}$  can be expressed at a given temperature (*T*) by the following equation.<sup>37</sup>

$$\Delta S_{\text{solv}} = \Delta C_p \ln(T/T_s) \quad (3)$$

where *T<sub>s</sub>* is the temperature at which there is no contribution of solvent to the hydrophobic entropy change and is equal to 112 °C (385 K).<sup>41</sup> If  $\Delta C_p = -0.19$  kcal mol<sup>−1</sup> K<sup>−1</sup>, *T* = 298 K, and *T<sub>s</sub>* = 385 K,  $\Delta S_{\text{solv}}$  for tubulin–TN16 interaction is 0.048 kcal mol<sup>−1</sup> K<sup>−1</sup>. Generally, it is hypothesized that a favorable desolvation entropy is directly correlated with the clustering of the hydrophobic group that results in solvent reorganization and release of water from the complex interface. For this system also, as discussed in the next section, the favorable  $\Delta S_{\text{solv}}$  correlates with the release of water of hydration for both ligands. Finally, the conformational entropy  $\Delta S_{\text{conf}}$  is calculated by rearranging eq 2 as

$$\Delta S_{\text{conf}} = \Delta S_{\text{tot}} - \Delta S_{\text{solv}} - \Delta S_{\text{r/t}} \quad (4)$$

The conformational entropy change is generally unfavorable for a complex formation process, as the binding is normally accompanied by the loss of configurational and rotational degrees of freedom for both the drug and the protein molecule. Therefore, a strategic design of ligand would try to restrain the ligands conformationally to minimize this penalty by bridging the difference in flexibility of uncomplexed and complexed states. Table 3 shows that although  $\Delta S_{\text{solv}}$  is the primary factor that makes the processes entropy driven,  $\Delta S_{\text{conf}}$  has considerable effect in modulating the value of  $\Delta S_{\text{tot}}$ . Here,  $\Delta S_{\text{conf}}$  suffers a minimal penalty for colchicine. To benchmark, the results were compared with the data for indanocine (Table 3), which is also known to bind at the colchicine binding site.<sup>42</sup> The conformational entropy value of TN16 closely resembles that of indanocine, and the two molecules have a structural resemblance (Figure 2). The similar changes in conformational entropy are reasonable as both the molecules possess significant rotational and vibrational degrees of freedom in the free state, which are suppressed to similar extents upon complexation. Colchicine exhibited a smaller change in conformational entropy than TN16 or indanocine, and this can be attributed to fewer losses of vibrational and rotational degrees of freedom upon formation of the complex. For tubulin–TN16 complex assembly, the unfavorable conformational entropy is largely compensated by a favorable solvent contribution that leads to a moderate entropic gain, which ultimately governs the binding reaction.

It is clear that tubulin–TN16 binding is associated with hydrophobic interaction that releases water molecules, freeing their degrees of freedom that were restricted otherwise. An additional contribution arises from the change in internal van der Waals packing and the change in hydrogen bonding interactions, which is reflected in a favorable enthalpy ( $\Delta H < 0$ )

of binding for TN16 compared to an unfavorable ( $\Delta H > 0$ ) contribution for colchicine.

**Computational Modeling and Simulations.** Each tubulin subunit consists of three domains, the N-terminal nucleotide-binding domain (residues 3–224), the intermediate domain, and the C-terminal domain (residues 261–383). The crystal structure of colchicine-bound tubulin includes the  $\alpha$ / $\beta$  heterodimer of tubulin with the drug bound at the interface of the  $\alpha$  and  $\beta$  subunits, although the major part of the interaction takes place with the intermediate domain of the  $\beta$  subunit with a partial overlap with the T5 loop of the  $\alpha$  subunit (Figure 1). The analysis of the structures (at the end of the simulation) of tubulin–colchicine and tubulin–TN16 complexes shows that TN16 spans between 6 and 18 Å, whereas colchicine spans between 15 and 28 Å from the center of mass of  $\beta$ -tubulin (Figure S1 of the Supporting Information), which reveals that TN16 is deeply buried (Figure 4a) in the  $\beta$  subunit. Being buried, it makes contacts with the secondary structural elements of the intermediate domain, establishing new interactions with the nucleotide-binding (N-terminal) domain, whereas colchicine is stabilized near the  $\alpha$ – $\beta$  interface (Figure 4a), showing much less access to the core of tubulin. The snapshots taken at the end of 10 ns simulations were superimposed with respect to tubulin to assess the relative positions of colchicine and TN16. It showed only limited overlap, the A-ring of colchicine overlapping with TN16 (Figure 4b). From the topological point of view, as well as from the dynamics in the uncomplexed states (Movies SM1 and SM2 of the Supporting Information), it is evident that TN16 is much more flexible than colchicine, which allows it to easily penetrate the interior of the  $\beta$  subunit (discussed later). TN16 binding mostly involves  $\beta$  strands, S4 (residues 134–140), S5 (residues 166–171), and S6 (residues 200–204); all three strands are at the core of the  $\beta$  subunit. Transient interactions are observed with the  $\alpha$  subunit with only Thr179 in the T5 loop being involved. As shown in Figure 4a, while the A-ring of TN16 is buried deep inside the pocket, the B- and C-rings of colchicine face outside, interacting with the T5 loop of the  $\alpha$  subunit.<sup>18</sup> The alteration of the T5 loop also occurs because of such interactions.

The colchicine binding site is endowed with features that allow it to accommodate many structurally unrelated drugs. The difference in the mode of binding of colchicine and TN16 in crystal structures and the complementary differences in the receptor's surface (Figure 4a) gave the initial clue about the plasticity of the binding pocket, which required follow-up investigations into its accessible conformational space. Molecular dynamics simulation has been used to understand the molecular movements in complexes of TN16 and colchicine with the  $\beta$  subunit (which provides most of the binding contacts to the ligand) and the dimer of tubulin. In the dimeric state, the interface is already in a sterically restricted situation; therefore, the conformational sampling using molecular

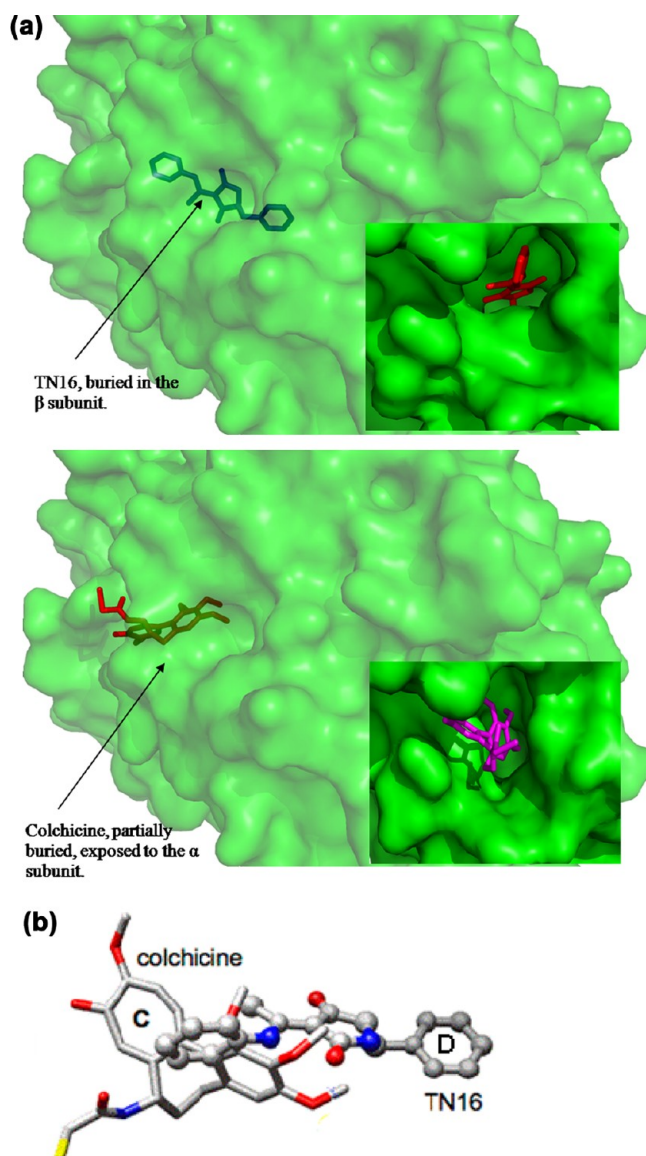


**Figure 4.** (a) Difference in the modes of binding of TN16 and colchicine. The two complexes, PDB entries 1SA0 and 3HKD, were first superimposed, and then the surface of one structure was taken. The surface has been kept translucent to show how colchicine and TN16 bind differently; one binds near the surface, and the other is more buried. The inset shows the actual surface with the drug viewed from the top (the side of the  $\alpha$  subunit). (b) Visualization of the orientation of the ligands obtained by superimposition of the tubulin molecule in PDB entries 1SA0 and 3HKD.

dynamics would demand a much longer computing time, and to some extent, the required length of simulation to witness such transitions is nontrivial to predict. To get an idea of the possible states that the binding pocket can access, an enhanced sampling was necessary within the window of the trajectories of this report, i.e.,  $\sim 10$  ns. There are several methods for accelerating the molecular dynamics, e.g., elevated temperature, potential scaling, etc., each of which is associated with some degree of unphysical situations and/or with chances of overall structural disruption.<sup>43,44</sup> Alternatively, in our protocol, the steric restriction was released by removing the  $\alpha$  subunit and sampling was performed. It was previously reported that tubulin at a low concentration can exist as a monomer and can also bind the ligand (e.g., colchicine),<sup>6</sup> but its structural validation

was not available until now. As a result, both the monomeric ( $\beta$  subunit) and the dimeric states of the molecule were used for the sampling of the conformational space.

**$\beta$  Subunit of Tubulin Complexed with Colchicine.** The simulation of the monomeric structure ( $\beta$  subunit) reveals the structural adaptability, showing faster movements of the ligand within the binding pocket and the complementary changes in the pocket's shape. In the crystal structure, colchicine is surrounded by loop T7 (residues 244–251) and helices H7 (residues 224–243) and H8 (residues 252–260) of the  $\beta$  subunit (Figure 5). During the simulation, the ligand crawls

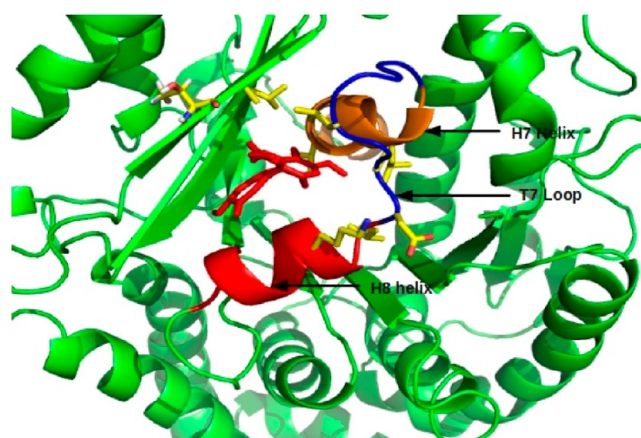


**Figure 5.** Environment of colchicine in the  $\beta$  subunit at the start of the simulation (corresponding to the crystal structure). The protein is shown as a pale green cartoon; the T7 loop is colored blue, and helices H7 and H8 are colored orange and pale red, respectively. Colchicine is represented as red sticks. The residues that fall within 4.5 Å of the drug are colored yellow.

along the binding site creating and breaking interactions with different residues. The movements of the ligand also induce complementary changes in the binding pocket shaping the pathway, as shown in Figure S2 of the Supporting Information, which distills out the inherent flexibility of the binding pocket. Colchicine moves farther from its initial binding site to occupy a new interaction site, the center of mass of the drug shifting by 8.1 Å. Several residues that lie within 4.5 Å of colchicine, such as Gly237, Val238, Thr239, Thr240, Arg243, Gln247, Asn249, Ala250, Val318, and Val354, are exclusive to the starting structure (Figure 5), but later during the simulation, residues such as Pro261, Leu313, Ile347, Asn361, Pro348, and Gly379 come closer to the drug, creating a more hydrophobic environment. The rmsd (root-mean-square deviation) gives an idea about the gross distortion or deviation of the structure compared with a reference frame, usually the starting structure. It also gives the average deviation for the whole structure at each time point of the simulation and measures how the structure changes over time. The rmsd of the tubulin backbone shows only marginal differences in magnitude, 2.7 and 3.2 Å at the end of 10 ns for the colchicine-bound and uncomplexed  $\beta$  subunit, respectively. The backbone (C $\alpha$ , C, and N) rmsd of the residues around the binding pocket ( $\sim 2.7$  Å) shows an almost stabilized structure for the uncomplexed tubulin, whereas an increase in the rmsd (from 3.3 to 3.7 Å) is observed during 7–10 ns of the simulations for the colchicine-bound structure; this indicates that the colchicine-bound complex undergoes more structural changes compared to the overall adjustment in the backbone.



The ligand moves away from the initial binding site to occupy a new location. To emphasize this, we looked at the surface accessibilities of the binding site. The initial binding site was defined by the residues that are within 4.5 Å of the drug at the start of the simulation; for the final binding site, the structure was taken after simulation for 10 ns. The accessible surface area (ASA) of the initial binding site increases over the simulation time from 269 to 505 Å<sup>2</sup> (Figure S3 of the Supporting Information).

To obtain an estimate of the ligand-induced change in intraprotein interactions, the total molecular mechanical energy ( $E_{\text{mm}}$ ) of the receptor was estimated (averaged over the last 5 ns of each trajectory). The value was  $-6182 \pm 82$  kcal/mol (colchicine bound) versus  $-6172 \pm 78$  kcal/mol (no ligand), indicating that there is a marginal change in the internal stability upon drug binding. There is thus little (or marginal) gain in internal packing induced by ligand binding.

As it was reported that the conformational change in the T7 loop is responsible for colchicine binding,<sup>18</sup> we studied the changes in the loop over the simulation period. At the starting point of the simulation, the T7 loop becomes stretched compared to its unbound conformation and the H7 and H8 helices move closer to  $\beta$  sheets S4 and S5, shrinking the binding cavity. Over the simulation, the T7 loop moves farther from the binding site to accommodate the movement of the drug, as a result of which helices H7 and H8 move away from each other. With a longer simulation time, colchicine moves closer to helix H8 (Figure S4a,b of the Supporting Information). For the  $\beta$  subunit without colchicine, the T7 loop becomes even more curved and relaxed during the simulation; as a result, two helices come closer to each other (Figure S4c of the Supporting Information).

**$\beta$  Subunit of the Tubulin–TN16 Complex.** Through a channel, TN16 is buried inside the  $\beta$  subunit, and there is no apparent change in the interacting residues over the simulation time, except some oscillation within the channel. The differences in the free and TN16-bound  $\beta$  subunit can be determined through the analysis of the rmsd and the total molecular mechanical energy changes of the respective systems. The overall backbone rmsd increases with time for both the free and drug-bound forms (2.7 and 3.14 Å, respectively, at the end of 10 ns). The deviation is also comparable for both considering the rmsd profile of the binding site residues (2.6 and 3.0 Å, respectively, at the end of 10 ns). Thus, the backbone shows greater deviation than the binding site, as opposed to the colchicine-bound complex that showed a greater change in the rmsd for the binding site. We did not find any appreciable difference in the energy profile of TN16 in the free and bound forms. However, the total molecular mechanical energy profile of the TN16-bound  $\beta$  subunit indicates that the receptor attains a higher stability ( $E_{\text{mm}} = -6262 \pm 81$  kcal/mol, averaged over the last 5 ns) compared to that of the colchicine complex ( $E_{\text{mm}} = -6182 \pm 82$  kcal/mol) and that of uncomplexed tubulin ( $E_{\text{mm}} = -6172 \pm 78$  kcal/mol). This shows that TN16 binding local adjustments of the protein chain leading to an enhanced internal packing, which contributes to the enthalpic stabilization of the overall complex.

It is further observed that although at the start of the simulation the conformations of the T7 loop and helices H7 and H8 are similar to that of the colchicine-bound  $\beta$  subunit, with the progression of time, the T7 loop does not extend or stretch as seen in the colchicine complex. Helices H7 and H8 move apart, but not as much as seen in the colchicine-bound

form, with the drug moving toward the H7 helix (Figure S5 of the Supporting Information).

**$\alpha\beta$  Tubulin Dimer Complexed with Colchicine.** The presence of the  $\alpha$  subunit restricts the movement of colchicine in the dimer–colchicine complex (Movie SM3 of the Supporting Information). As tubulin–colchicine interaction is entropy-driven (Table 1), one needs to identify the factors leading to the gain in entropy. We use the rmsf (root-mean-square fluctuations) to describe the local flexibility of the molecule, calculated using the atomic fluctuations of the structures averaged over all the frames of the trajectory. The rmsf measures the flexibility of individual residues, while the rmsd is an indicator for gross structural changes. The rmsf of backbone atoms (C $\alpha$ , C, and N) for each residue, over the simulation trajectories (Figure S6 of the Supporting Information), shows an almost similar trend for both complexes, except in the terminal ends of tubulin. The structure bound to TN16 shows more deviation (rmsd) in the backbone than the dimer bound to colchicine (Figure 6), taking the crystal structures as

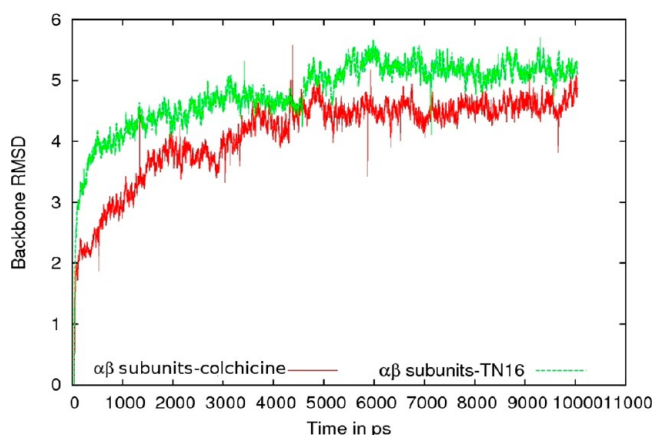


**Figure 6.** Backbone rmsd (Å) of the  $\alpha\beta$  dimer in complexation with colchicine and TN16, showing the overall rmsd change to be greater for the TN16 complex.

the reference points in each case. When the rmsd of an individual drug molecule is considered, colchicine shows greater changes than TN16, although a sharp peak in the profile for TN16 is seen around 3 ns, which can be attributed to the translation taking place between the drug and the two leucines (242 and 252) in the  $\beta$  subunit (Figure 7). The backbone rmsd for the overall structure increases for both the bound and the free receptor and is greater than the change observed in the colchicine-bound  $\beta$  subunit (4.8 Å for both, at the end of 10 ns). However, from the rmsd profile of the binding site residues, it is clear that colchicine binding causes a greater change in the  $\beta$  subunit than in the dimer (Figure S7 of the Supporting Information; rmsd values after 10 ns are 3.7 and 2.7 Å, respectively).

To investigate the movement of the drug inside the tubulin dimer, we looked at the ASA values of binding sites in the initial and final structures. As the binding site consists mainly of the  $\beta$  subunit, we restrict ourselves to residues of this subunit only. The ASA value is quite low for the initial binding site [ $\sim 250$  Å<sup>2</sup> (Figure S3 of the Supporting Information)]. On the other hand, the residues that constitute the final interaction site had a larger starting value ( $\sim 700$  Å<sup>2</sup>) that finally converged to 650 Å<sup>2</sup>. This feature is reflected in the rmsd change as well; the residues that constitute the initial binding site show less deviation than

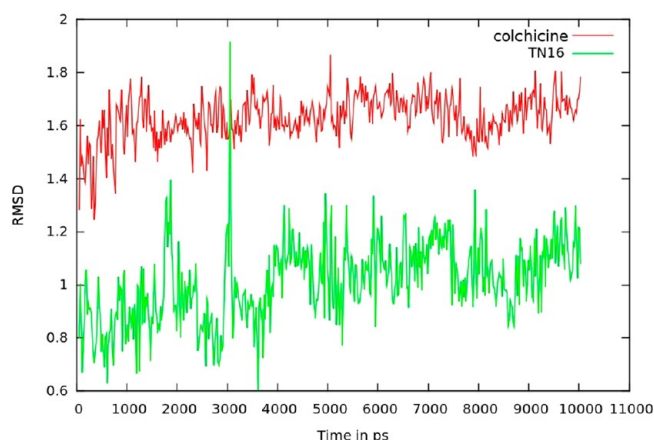


**Figure 7.** rmsd (Å) of the ligands alone, colchicine, and TN16 over time. The overall structural deviation is greater for colchicine than for TN16, although a sharp peak is observed for TN16 around 3 ns, which is attributed to the swinging movement of the molecule.

those involved in the final binding site (rmsd values of 2.7 and 3.1 Å, respectively). The conformational changes in the T5 loop (residues 173–182) of the  $\alpha$  subunit along with helices H7 and H8 and the T7 loop in the  $\beta$  subunit of the colchicine-bound dimer were also studied. After simulation, the T7 loop moves into the colchicine binding site as the drug translates toward the T5 loop (Figure S8a,b of the Supporting Information). During the simulation, the two helices moved apart.

**$\alpha\beta$  Tubulin Dimer Complexed with TN16.** TN16 consists of three rings [D–F (Figure 2)]; the D-ring flips between two leucine residues (242 and 252), and the F-ring is found tossing among hydrophobic residues (Leu248, Leu255, Met259, Ala317, Val318, and Ile377) of the  $\beta$  subunit, thus generating a rocking movement of the drug (Movies SM4 and SM5 of the Supporting Information). This observation is astonishing as TN16 bound to the  $\beta$  subunit (monomer) shows less movement (only ring flipping was observed) than what is seen in the dimer, possibly because the exposure of the hydrophobic binding pocket to the solvent in the monomer makes the cavity opening more constricted, restricting the movement of the ligand. In the dimer, the drug movement is mostly observed within the first 4 ns and then the structure becomes stabilized. Although on its own TN16 is flexible (Movie SM2), the flexibility is not manifested in the binding region of the complex. However, the channel allows the molecule to rock as a whole (Movies SM4 and SM5 of the Supporting Information), contributing to the entropic stabilization of the complex, in agreement with the experimental data.

The dynamics of loops T5 and T7 have been investigated as they are very crucial for colchicine binding and thus might also have an impact on TN16 binding. In the starting structure, the drug occupies the cavity vacated by the loop (Figure S8c of the Supporting Information); however, as the simulation progresses, little movement of the drug toward the interface is observed, and as a consequence, marginal bending of the T5 loop in the  $\alpha$  subunit occurs. No appreciable movement of the T7 loop was noticed as it retains its original position; this is expected, as the drug moves very little from its initial location and occupies most of the binding cavity. This is in contrary to that observed for colchicine binding, where the drug moves more toward the interface (T5 loop) and the T7 loop occupies more of the colchicine initial binding site (Figure S8d of the

Supporting Information). The dimer–colchicine structure is less stable than the dimer–TN16 complex as seen for the complexes involving the monomer as well (Figure S9 of the Supporting Information;  $E_{\text{mm}} = -11932 \pm 117$  kcal/mol for the dimer–colchicine structure vs  $E_{\text{mm}} = -12065 \pm 116$  kcal/mol for the dimer–TN16 structure, averaged over the last 5 ns).

## DISCUSSION

Experimental data show that colchicine and TN16 both bind to tubulin because of a very favorable entropic contribution to binding, and this contribution is greater for colchicine; additionally, there are differences in the conformational and solvation components of entropy. The  $\Delta H$  for colchicine binding is unfavorable, but for TN16 binding, it is favorable. Crystallographic data showed a considerable difference in the binding modes of these two ligands. The mechanistic insight into these observations is obtained from the molecular dynamics simulations. TN16 experiences a “cozier” binding being deeply buried in the pocket that is shaped like a channel. The steric factor (originating from the shape of the ligand) prevents colchicine from gaining access deep inside the binding pocket, whereas TN16 can easily be molded to fit into the channel (see Movies SM4 and SM5 of the Supporting Information). The cozy fit is reflected in the enhanced van der Waals stabilization ( $\Delta E_{\text{vdw}} = -47$  kcal/mol, compared to  $-13$  kcal/mol for colchicine), which is in agreement with the favorable  $\Delta H$  for TN16 binding. Colchicine is found to continuously switch between interaction modes, not relying on any one of them for its binding, leading to an unfavorable  $\Delta H$ . The binding of colchicine to tubulin is favored by entropy ( $-T\Delta S = -19.6$  kcal/mol) (Table 1), the enthalpic contribution being unfavorable. In contrast, TN16 binding is favored by both enthalpy and entropy, although the entropic component is still more significant ( $-T\Delta S \sim -6$  kcal/mol) than enthalpy ( $-1.7$  kcal/mol). The gain in enthalpic stabilization results primarily from the change in electrostatic and van der Waals interactions, whereas entropic stabilization may originate from the flexibility of the structure as well as the release of interfacial water molecules, freeing the degrees of their motion.<sup>45</sup> In general, formation of protein–ligand complexes provides an entropic benefit if water molecules are released from the interface upon binding.<sup>46–48</sup> This is an important aspect facilitating biomolecular recognition.<sup>47,48</sup> Solvation of the uncomplexed colchicine and TN16 using explicit (TIP3P) water molecules reveals that colchicine can accommodate approximately 27 molecules within a 4 Å cutoff (first hydration layer<sup>46</sup>), whereas for TN16, this number is  $\sim 20$ . Because both ligands are completely sequestered from the solvent when they are complexed in the dimer, the number of released water molecules would be much higher for colchicine than for TN16, i.e., more entropic stabilization for colchicine binding. This is also apparent from the  $\Delta S_{\text{solv}}$  data (Table 3) that show that one of the major components of the higher stability of the colchicine complex is the entropy of desolvation.

The greater entropic contribution for colchicine binding also correlates with the different binding conformations it can attain, as revealed in the trajectory of the  $\beta$  subunit–colchicine complex. Sampling of such a large conformational space is not observed in the 10 ns simulation of the dimer–colchicine complex, as conformational modulation can take place more slowly within the dimer, at a time scale beyond the scope of this study. As mentioned earlier, colchicine continuously switches its interactions with the receptor residues during its drive across



the binding pocket, which is analogous to the flying trapeze; although the drug cannot translate much within the cavity of the dimer, a number of transient interactions can occur between the drug and residues of the receptor, clearly seen in Movie SM3 of the Supporting Information. It is not a particular set of interactions that stabilizes colchicine in the binding site; rather, the interactions change continuously (Movie SM3 of the Supporting Information), and the inherent motion of colchicine within the binding cavity is responsible for the high entropy value. Compared to colchicine, TN16 penetrates into the core of the receptor and thus shares the comfort zone created by the internal hydrophobic packing of the receptor. It can be seen in the Movie SM4 of the Supporting Information that the ligand can bend easily to be inserted into the cavity and can rock like a swing cradle, where its D-ring is in contact with few leucine residues and the F-ring with hydrophobic residues leading to a greater hydrophobic packing. Movie SM5 of the Supporting Information shows that this results in almost complete burial of the ligand in the binding groove, which then takes a shape that is completely different from that accompanying colchicine binding.

For TN16 binding, there is a fine-tuning between enthalpy and entropy. It packs better inside the deep groove and gains much from van der Waals interactions ( $\Delta E_{\text{vdw}} = -47$  kcal/mol, compared to  $-13$  kcal/mol for colchicine). There is also an overall gain in the molecular mechanical energy of the receptor itself, all contributing to the enthalpic gain for TN16 binding, supporting the experimental result (Table 1). A better packing of the ligand, however, reduces its flexibility, suggesting that by merely reducing the bulkiness and/or making a better fit into the pocket one cannot make a drug more potent, as it can affect the entropic component and thus reduce the overall level of stabilization of the ligand. Thus, optimizing the balance between enthalpy and entropy could be a rational approach in the quest for a tight binding ligand.

Rigorous investigations over the past few decades using techniques like QSAR, screening, docking, and other in silico methodologies have yielded a pool of potent colchicine binding site agents,<sup>49</sup> but most of these attempts ignored the role of the inherent flexibility of the binding pocket and the induced conformational changes in both the ligand and the receptor. Our investigation offers a plausible explanation for these compounds not producing a lead compound in the in vitro and/or in vivo tests. The flexibility of the colchicine binding site is found to be the most critical factor for switching between different mechanisms for accommodating the two different ligands, balancing flexibility as well as stabilizing interactions. Dorleansa et al. have recently dissected the colchicine domain into two parts, the core colchicine binding site and an additional pocket.<sup>18</sup> The flexibility of the domain changes depending on the drug binding position. TN16 has a flexible structure compared to colchicine, allowing it to penetrate inside the core of the  $\beta$  subunit and interact efficiently with an additional binding pocket. Very little movement or fluctuation of the additional binding cavity is observed after accommodating the drug, which clearly indicates the conformational constraints of the binding site, although some minor translation of TN16 within the binding cavity takes place because of the flipping of the D- and F-rings. Compared to the TN16 binding site, the core colchicine binding site is much more flexible. When only the  $\beta$  subunit (monomer) is considered, colchicine moves much faster (Figure S1 of the Supporting Information) to occupy a new interaction site. The restriction of colchicine

movement inside the dimer implies the importance of the  $\alpha$  subunit for drug binding. It is understood that the  $\alpha$  subunit imposes constraints impeding the approach of colchicine toward the binding site during the association reaction. This makes the exit and entry of the drug difficult, which is why the binding is poorly reversible with very slow on and off rates in the case of the dimer.

## CONCLUSIONS

In this investigation, the thermodynamics of two structurally different ligands that compete for the same binding site of the  $\alpha$ - $\beta$  interface of tubulin have been studied by ITC measurements, and the complementary molecular dynamics simulations have provided atomistic insight into the binding mechanisms. There are a few salient features. (i) The colchicine binding site is inherently flexible in nature, and depending upon the drug to which it binds, it can adopt drastic changes in its shape. (ii) The ability of a drug to access deep inside the colchicine binding site depends on the steric factor (bulkiness) and the flexibility of the molecule. TN16 can access the region where colchicine cannot enter, leading to a difference in the complex structures. (iii) The effects of enthalpy and entropy are complementary for these two ligands; hydrophobic packing makes the  $\Delta H$  favorable for TN16, but at the cost of slightly diminishing  $\Delta S$ , and transient interactions give an unfavorable  $\Delta H$  for colchicine, simultaneously causing an entropic gain. (iv)  $\Delta S_{\text{solv}}$  is critical for binding and is correlated with the release of water of hydration.

Entropy is a crucial factor in stabilizing the binding of colchicine and TN16 to tubulin. The common practice for the improvement of binding affinities is to add more pharmacophoric attachment points. However, in the realm of tubulin, such a process could lead to a possible decrease in the entropy of binding, thus resulting in the destabilization of the protein-drug interaction. This provides lessons for future design strategies.

## ASSOCIATED CONTENT

### Supporting Information

Span of the two drugs relative to the center of mass of the  $\beta$  subunit (Figure S1), structures from different time points of the simulation for the  $\beta$  subunit–colchicine complex (Figure S2), the ASA (accessible surface area, in square angstroms) changes of the dimer and  $\beta$  subunit bound to colchicine, over the period of the simulation (Figure S3), the dynamics of the T7 loop and helices H7 of H8 in the  $\beta$  subunit, in the free state and bound to colchicine, over the simulation time (Figure S4), the location of TN16, the T7 loop, and helices H7 and H8 in the  $\beta$  subunit (Figure S5), the rmsf of the dimer complexes bound to colchicine and TN16 over the simulation period (Figure S6), the binding site rmsd (angstroms) over the simulation time for both the dimer and  $\beta$  subunit bound to colchicine (Figure S7), the dynamics of loops T5 and T7 and helices H7 and H8 for the dimer bound to colchicine and TN16 (Figure S8), the energy profile (kilocalories per mole) for the dimer bound to TN16 and colchicine (Figure S9), the dynamics of drugs (colchicine and TN16, respectively) alone (Movies SM1 and SM2), the dynamics of colchicine and TN16 (top and side views) in the dimer (Movies SM3–SM5, respectively), and a list of trajectories (Table S1). This material is available free of charge via the Internet at <http://pubs.acs.org>.

# AUTHOR INFORMATION

## Corresponding Author

\*B.B.: Department of Biochemistry, Bose Institute, Centenary Campus, P-1/12, CIT Scheme VII M, Kolkata 700054, India; fax, 91-33-2355-3886; telephone, 91-33-2355-0256; e-mail, bablu@boseinst.ernet.in. S.G.D.: Bioinformatics Centre, Bose Institute, Centenary Campus, P-1/12, CIT Scheme VII M, Kolkata 700054, India; fax, 91-33-2355-3886; telephone, 91-33-2355-0256; e-mail, sgd@boseinst.ernet.in.

## Author Contributions

S.C. and D.C. have contributed equally to this work.

## Funding

This work was supported by grants from the Department of Atomic Energy (DAE), as a Raja Ramanna Fellowship, to B.B. and the Indo-French Centre for the Promotion of Advanced Research (IFCPAR) to P.C. S.C. and D.C. acknowledge the Council of Scientific and Industrial Research (CSIR) and IFCPAR, respectively, for research fellowships. P.C. is a recipient of the JC Bose National Fellowship from the Department of Science and Technology (DST).

## Notes

The authors declare no competing financial interest.

# REFERENCES

- (1) Jordan, M. A., and Wilson, L. (2004) Microtubules as a target for anticancer drug. *Nat. Rev. Cancer* 4, 256–265.
- (2) Singh, P., Rathinasamy, K., Mohan, R., and Panda, D. (2008) Microtubule assembly dynamics: An attractive target for anticancer drugs. *IUBMB Life* 60, 368–375.
- (3) Kanakkanthara, A., Wilmes, A., O'Brate, A., Escuin, D., Chan, A., Gyrezi, A., Crawford, J., Rawson, P., Kivell, B., Northcote, P. T., Hamel, E., Giannakakou, P., and Miller, J. H. (2011) Peloruside- and laulimalide-resistant human ovarian carcinoma cells have  $\beta$ II-tubulin mutations and altered expression of  $\beta$ II- and  $\beta$ III-tubulin isotypes. *Mol. Cancer Ther.* 10, 1419–1429.
- (4) Begaye, A., Trostel, S., Zhao, Z., Taylor, R. E., Schriemer, D. C., and Sackett, D. L. (2011) Mutations in the  $\beta$ -tubulin binding site for peloruside A confer resistance by targeting a cleft significant in side chain binding. *Cell Cycle* 10, 3387–3396.
- (5) Orr, G. A., Verdier-Pinard, P., McDaid, H., and Horwitz, S. B. (2003) Mechanisms of taxol resistance related to microtubules. *Oncogene* 22, 7280–7295.
- (6) Banerjee, S., Chakrabarti, G., and Bhattacharyya, B. (1997) Colchicine binding to tubulin monomers: A mechanistic study. *Biochemistry* 36, 5600–5606.
- (7) Rosner, M., Capraro, H. G., Jacobson, A. E., Atwell, L., Brossi, A., Iorio, M. A., Williams, T. H., Sik, R. H., and Chignell, C. F. (1981) Biological effects of modified colchicine. Improved preparation of 2-demethylcolchicine, 3-demethylcolchicine, and (+)-colchicine and reassignment of the position of the double bond in dehydro-7-deacetamidocolchicine. *J. Med. Chem.* 24, 257–261.
- (8) Andreu, J. M., and Timasheff, S. N. (1982) Interaction of tubulin with single ring analogues of colchicine. *Biochemistry* 21, 534–543.
- (9) McClure, W. O., and Paulson, J. C. (1977) The interaction of colchicine and some related alkaloids with rat brain tubulin. *Mol. Pharmacol.* 13, 560–575.
- (10) Fitzgerald, T. J. (1976) Molecular features of colchicine associated with antimitotic activity and inhibition of tubulin polymerization. *Biochem. Pharmacol.* 25, 1383–1387.
- (11) Bane, S., Puett, D., MacDonald, T. L., and Williams, R. C., Jr. (1984) Binding to tubulin of the Colchicine Analog 2-Methoxy-5-(2',3',4'-trimethoxyphenyl) tropone. *J. Biol. Chem.* 259, 7391–7398.
- (12) Ray, K., Bhattacharyya, B., and Biswas, B. B. (1981) Role of B-ring of colchicine in its binding to tubulin. *J. Biol. Chem.* 256, 6241–6244.

- (13) Hastie, S. B., Williams, R. C., Puett, D., and MacDonald, T. L. (1989) The binding of isocolchicine to tubulin. *J. Biol. Chem.* 264, 6682–6686.
- (14) Hastie, S. B. (1989) Spectroscopic and kinetic features of allocolchicine binding to tubulin. *Biochemistry* 28, 7753–7760.
- (15) Chakrabarti, G., Sengupta, S., and Bhattacharyya, B. (1996) Thermodynamics of colchicinoid-tubulin interactions. *J. Biol. Chem.* 271, 2897–2901.
- (16) Pyles, E. A., and Bane Hastie, S. (1993) Effect of B-ring and the C-7 substitution on the kinetics of colchicine tubulin association. *Biochemistry* 32, 2329–2336.
- (17) Bhattacharyya, B., Panda, D., Gupta, S., and Banerjee, M. (2008) Anti-Mitotic Activity of Colchicine and the Structural Basis for Its Interaction with Tubulin. *Med. Res. Rev.* 28, 155–183.
- (18) Dorleans, A., Gigant, B., Ravelli, R. B., Mailliet, P., Mikol, V., and Knossow, M. (2009) Variations in the colchicine-binding domain provide insight into the structural switch of tubulin. *Proc. Natl. Acad. Sci. U.S.A.* 106, 13775–13779.
- (19) Xu, K., Schwarz, P. M., and Luduena, R. F. (2002) Interaction of nocodazole with tubulin isotypes. *Drug Dev. Res.* 55, 91–96.
- (20) Chetrit, B. E., and Levy, M. (1998) Colchicine: 1998 Update. *Semin. Arthritis Rheum.* 28, 48–59.
- (21) Ravelli, R. B., Gigant, B., Curmi, P. A., Jourdain, I., Lachkar, S., Sobel, A., and Knossow, M. (2004) Insight into tubulin regulation from a complex with colchicine and a stathmin-like domain. *Nature* 428, 198–202.
- (22) Adams, J., and Elliott, P. J. (2000) New agents in cancer clinical trials. *Oncogene* 19, 6687–6692.
- (23) Beaugerard, D. A., Hill, S. A., Chaplin, D. J., and Brindle, K. M. (2001) The susceptibility of tumors to the antivascular drug combretastatin A4 phosphate correlates with vascular permeability. *Cancer Res.* 61, 6811–6815.
- (24) Rustin, G. J., Galbraith, S. M., Anderson, H., Stratford, M., Folkes, L. K., Sena, L., Gumbrell, L., and Price, P. M. (2003) Phase I clinical trial of weekly combretastatin A4 phosphate: Clinical and pharmacokinetic results. *J. Clin. Oncol.* 21, 2815–2822.
- (25) Yamamoto, K., Noda, K., Yoshimura, A., Fukuoka, M., Furuse, K., and Niitani, H. (1998) Phase I study of E7010. *Cancer Chemother. Pharmacol.* 42, 127–134.
- (26) Pannacchiulli, I., Ballarino, P., Castello, G., Arboscello, E., Botta, M., Tredici, S., and Lerza, R. (1999) In vitro toxicity of taxol based anticancer drug combinations on human hemopoietic progenitors. *Anticancer Res.* 19, 409–412.
- (27) Arai, T. (1983) Inhibition of microtubule assembly in vitro by TN16, a synthetic antitumor drug. *FEBS Lett.* 155, 273–276.
- (28) Lin, C. M., and Hamel, E. (1981) Effects of inhibitors of tubulin polymerization on GTP hydrolysis. *J. Biol. Chem.* 256, 9242–9245.
- (29) Banerjee, A., and Luduena, R. F. (1987) Kinetics of association and dissociation of colchicine-tubulin complex from brain and renal tubulin. Evidence for the existence of multiple isotypes of tubulin in brain with differential affinity to colchicine. *FEBS Lett.* 219, 103–107.
- (30) Case, D. A., Cheatham, T., Darden, T., Gohlke, H., Luo, R., Merz, K. M., Jr., Onufriev, A., Simmerling, C., Wang, B., and Woods, R. (2005) The Amber biomolecular simulation programs. *J. Comput. Chem.* 26, 1668–1688.
- (31) Tsui, V., and Case, D. A. (2000) Molecular dynamics simulations of nucleic acids with a generalized Born solvation model. *J. Am. Chem. Soc.* 122, 2489–2498.
- (32) Cavallo, L., Kleinjung, J., and Fraternali, F. (2003) POPS: A fast algorithm for solvent accessible surface areas at atomic and residue level. *Nucleic Acids Res.* 31, 3364–3366.
- (33) Dundas, J., Ouyang, Z., Tseng, J., Binkowski, A., Turpaz, Y., and Liang, J. (2006) CASTp: Computed atlas of surface topography of proteins with structural and topographical mapping of functionally annotated residues. *Nucleic Acids Res.* 34, W116–W118.
- (34) Schön, A., Madani, N., Smith, A. B., Lalonde, J. M., and Freire, E. (2011) Some binding-related drug properties are dependent on thermodynamic signature. *Chem. Biol. Drug Des.* 77, 161–165.

- (35) Murphy, K. P., Bhakuni, V., Xie, D., and Freire, E. (1992) Molecular basis of cooperativity in protein folding. III. Structural identification of cooperative folding units and folding intermediates. *J. Mol. Biol.* 227, 293–306.
- (36) Hubbard, S. J., and Thornton, J. M. (1996) *NACCESS Computer Program*, version 2.1.1, Department of Biochemistry and Molecular Biology, University College London, London.
- (37) Perozzo, R., Folkers, G., and Scapozza, L. (2004) Thermodynamics of protein ligand interactions: History, presence, and future aspects. *J. Recept. Signal Transduction Res.* 24, 1–52.
- (38) Freire, E. (2008) Do enthalpy and entropy distinguish first in class from best in class? *Drug Discovery Today* 13, 869–874.
- (39) Chakraborti, S., Das, L., Kapoor, N., Das, A., Dwivedi, V., Poddar, A., Chakraborti, G., Janik, M., Basu, G., Panda, D., Chakraborti, P., Suroliya, A., and Bhattacharyya, B. (2011) Curcumin recognizes a unique binding site of tubulin. *J. Med. Chem.* 54, 6183–6196.
- (40) Kauzmann, W. (1959) Some factors in the interpretation of protein denaturation. *Adv. Protein Chem.* 14, 1–63.
- (41) Baldwin, R. L. (1986) Temperature dependence of the hydrophobic interaction in protein folding. *Proc. Natl. Acad. Sci. U.S.A.* 83, 8069–8072.
- (42) Das, L., Gupta, S., Dasgupta, D., Poddar, A., Janik, M. E., and Bhattacharyya, B. (2009) Binding of indanocine to the colchicine site on tubulin promotes fluorescence, and its binding parameters resemble those of the colchicine analogue AC. *Biochemistry* 48, 1628–1635.
- (43) Sugita, Y., and Okamoto, Y. (1999) Replica-exchange molecular dynamics method for protein folding. *Chem. Phys. Lett.* 314, 141–151.
- (44) Hamelberg, D., Mongan, J., and McCammon, J. A. (2004) Accelerated molecular dynamics: A promising and efficient simulation method for biomolecules. *J. Chem. Phys.* 120, 11919–11929.
- (45) Ross, P. D., and Subramanian, S. (1981) Thermodynamics of protein association reactions: Forces contributing to stability. *Biochemistry* 20, 3096–3102.
- (46) Ghosh Dastidar, S., and Mukhopadhyay, C. (2003) Structure, dynamics and energetics of water at the surface of a small globular protein: A molecular dynamics simulation. *Phys. Rev. E* 68, 021921.
- (47) Dunitz, J. D. (1994) The entropic cost of bound water in crystals and biomolecules. *Science* 264, 670.
- (48) Baron, R., Setny, P., and McCammon, J. A. (2010) Water in cavity-ligand recognition. *J. Am. Chem. Soc.* 132, 12091–12097.
- (49) Zhang, S. X., Feng, J., Kuo, S. C., Brossi, A., Hamel, E., Tropsha, A., and Lee, K. H. (2000) Antitumor agents. 199. Three-dimensional quantitative structure-activity relationship study of the colchicine binding site ligands using comparative molecular field analysis. *J. Med. Chem.* 43, 167–176.